Thermostability and Ca^{2+} Binding Properties of Wild Type and Heterologously Expressed PsbO Protein from Cyanobacterial Photosystem II†

Bernhard Loll,*,‡,§ Gisa Gerold,‡,§,||,⊥ Daria Slowik,# Wolfgang Voelter,|| Christiane Jung,▽ Wolfram Saenger,‡ and Klaus-Dieter Irrgang*,#

Department of Chemistry/Crystallography, Free University Berlin, 14195 Berlin, Germany, Physical Biochemistry, Institute for Physiological Chemistry, Eberhard Karls University Tübingen, 72076 Tübingen, Germany, Institute of Chemistry/Max-Volmer-Laboratories for Biophysical Chemistry, Technical University Berlin, 10623 Berlin, Germany, and Max Delbrück Center for Molecular Medicine, Berlin Buch, Robert-Rössle-Strasse 10, 13125 Berlin, Germany

Received November 11, 2004; Revised Manuscript Received January 21, 2005

ABSTRACT: Oxygenic photosynthesis takes place in the thylakoid membrane of cyanobacteria, algae, and higher plants. Initially light is absorbed by an oligomeric pigment−protein complex designated as photosystem II (PSII), which catalyzes light-induced water cleavage under release of molecular oxygen for the biosphere on our planet. The membrane-extrinsic manganese stabilizing protein (PsbO) is associated on the lumenal side of the thylakoids close to the redox-active $(Mn)_4Ca$ cluster at the catalytically active site of PSII. Recombinant PsbO from the thermophilic cyanobacterium *Thermosynechococcus elongatus* was expressed in *Escherichia coli* and spectroscopically characterized. The secondary structure of recombinant PsbO (recPsbO) was analyzed in the absence and presence of Ca^{2+} using Fourier transform infrared spectroscopy (FTIR) and circular dichroism spectropolarimetry (CD). No significant structural changes could be observed when the PSII subunit was titrated with Ca^{2+} in vitro. These findings are compared with data for spinach PsbO. Our results are discussed in the light of the recent 3D-structural analysis of the oxygen-evolving PSII and structural/thermodynamic differences between the two homologous proteins from thermophilic cyanobacteria and plants.

Photosystem II (PSII)[1] harnesses sunlight to split water into molecular oxygen and protons. PSII is a multi-subunit pigment−protein complex composed of membrane-intrinsic and membrane-extrinsic subunits harboring a number of different cofactors (chlorophyll *a* (Chl*a*), pheophytin *a*, non-heme Fe^{2+}, plastoquinones, carotenoids, Mn cluster, Ca^{2+}, and Cl^-). The core antenna proteins CP43 and CP47 are located at the periphery of the reaction center subunits D1 and D2; cytochrome *b*-559 and at least 10 other low molecular mass polypeptides of largely unknown function are embedded in the thylakoid membrane, whereas PsbO, PsbU, and PsbV (cytochrome *c*-550) are membrane-extrinsic and attached at the lumenal side of the PSII core. Water cleavage is catalyzed by a redox-active $(Mn_4)Ca$ cluster. Additionally, one Cl^- could be essential for the redox cycle (*1*).

Whereas PsbO is present in all oxygenic photoautotrophic organisms, the cyanobacterial PsbU and PsbV are functionally replaced by PsbQ and PsbP in green algae and in higher plants (*2*). Even though the cyanobacterial PsbO reveals deletions and insertions in its primary structure, there is a moderate similarity of 40−50% between cyanobacteria and higher plants (*2*−*4*). Limited proteolysis of PsbO isolated from various organisms results in different degradation products (*5*). Structural predictions, based on UV−CD spectropolarimetry (*6*−*8*) and Fourier transform infrared spectroscopy (FTIR) (*6*, *9*−*12*), revealed a high β-sheet content, whereas other spectroscopic studies suggested a "natively unfolded" structure (*6*). Furthermore PsbO exhibits pronounced pH-dependent structural changes (*9*, *13*). These results and other typical features of PsbO were discussed by Shutova et al. suggesting a "molten globule" structure with a hydrophobic β-sheet structure (*14*). Recent preliminary NMR studies on the overexpressed isolated protein from *Thermosynechococcus elongatus* led the authors to suggest that PsbO rather consists of a hydrophobic core and highly flexible domains (*15*). The recently published X-ray structures of *T. elongatus* (*16*, *17*) and *Thermosynechococcus*

† This study was supported in part by Sonderforschungsbereich 498 (Project A4 and C7), EU Grant HPRI-CT-1999-00022, and Fonds der Chemischen Industrie.

* Corresponding authors. B.L.: Department of Chemistry/Crystallography, Free University Berlin, 14195 Berlin, Takustrasse 6, Germany. Phone: 49-30-838 56758. Fax: 49-30-838 56702. E-mail: loll@chemie.fu-berlin.de. K.-D.I.: Institute of Chemistry/Max-Volmer-Laboratories for Biophysical Chemistry, Technical University Berlin, 10623 Berlin, Strasse des 17. Juni 135, Germany. Phone: 49-30-314-23396. Fax: 49-30-314-21122. E-mail: irrg0532@mailbox.tu-berlin.de.

‡ Free University Berlin.

§ These authors contributed equally to this work.

|| Eberhard Karls University Tübingen.

⊥ Present address: MPI for Infection Biology, Campus Charité Mitte, D-10117 Berlin, Germany.

Technical University Berlin.

▽ Max Delbrück Center for Molecular Medicine.

[1] Abbreviations: Chl*a*, chlorophyll *a*; CD, circular dichroism; EGTA, ethylene glycol bis(β-aminoethyl ether)-*N*,*N*,*N*′,*N*′-tetraacetic acid; Θ, ellipticity; FTIR, Fourier transform infrared spectroscopy; GdmCl, guanidinium-HCl; IPTG, isopropyl β-D-thiogalactopyranoside; MALDI-TOF, matrix assisted laser desorption ionization time of flight mass spectrometry; MES, 2-(*N*-morpholino)ethanesulfonic acid; PCR, polymerase chain reaction; PS, photosystem; recPsbO, recombinant PsbO; SDS, sodium dodecyl sulfate; wt, wild type.

10.1021/bi047614r CCC: $30.25
Published on Web 03/05/2005

vulcanus (*18*) at medium resolutions showed that PsbO is in immediate vicinity to PsbU and interacts with the lumenal domains of D1, D2, and CP47, supported by cross-linking studies (*19*, *20*). It seems to regulate the substrate accessibility (*21*), but it does not directly ligate the Mn cluster (*22*). PsbO forms a hollow cylinder, that mainly consists of β-sheets featuring a length of 35 Å and a diameter of 15 Å. It resembles a β-barrel like structure in agreement with a proposal that this subunit could form a channel-like structure (*9*, *16*−*18*, *23*). Proton wires provided by PsbO between the catalytic site of water oxidation and the thylakoid lumen (*9*) and channel-like structures on the donor side have been earlier suggested in refs *24* and *25*.

Several possible functions were proposed for PsbO: it maintains the redox-active Mn cluster in the active site (*26*, *27*), and affects its stability as well as the S-state transitions (*28*). Δ*psbO* mutants from *Synechocystis* sp. PCC6803 reveal modified $Y_z^{\bullet}$ reduction kinetics (*29*) as well as alterations in the Mn photoligation during assembling of the PSII complex (*30*). Furthermore, they show decreased oxygen evolution capacity and their PSII is light sensitive (*30*−*33*). Therefore this subunit is also referred to as the manganese stabilizing protein. In vitro PsbO can be removed from cyanobacterial and plant PSII by high $CaCl_2$ concentrations sometimes accompanied by a loss of two manganese ions of the tetrameric Mn cluster (*34*), but see ref *35*. The oxygen-evolving activity can be largely restored under nonphysiological Ca^{2+} and Cl^- concentrations (*34*). Its rebinding restores the oxygen-evolution activity and stability of the active site (*1*, *3*, *4*). Whether PsbO specifically binds Ca^{2+} is not yet clear (*36*−*38*). It could provide an appropriate ionic environment (Ca^{2+}, Cl^-) for the oxygen-evolving complex. Recently, Ca^{2+} dependent conformational changes within PsbO from spinach were studied by FTIR (*38*). Conclusions from these data disagree with those drawn from EPR data on intact PSII and that depleted of the extrinsic subunits (*36*). An additional function of PsbO from thermophilic cyanobacteria discussed is that it may play a stabilizing role on PSII leading to an increased thermostability of the holocomplex (*6*, *39*).

In the work presented here, we describe the overexpression of *psbO* in *Escherichia coli* and characterization of the gene product by biochemical and spectroscopic methods. As there is no three-dimensional structure for PsbO available at the atomic level, we applied UV−CD spectropolarimetry to analyze its secondary structure elements. We compare the UV−CD and FTIR spectra of wild type (wt) PsbO, chemically removed from PSII, with those of recPsbO. On the basis of these spectroscopic data, we conclude that recPsbO is correctly folded and can reconstitute a quasi-native PSII core complex. To elucidate probable Ca^{2+} binding site(s), recPsbO was titrated in the presence of $CaCl_2$, followed by UV−CD and FTIR spectroscopy, but no significant changes in the secondary structure could be observed. Furthermore, the thermostability was studied by far UV−CD and revealing an increased portion of secondary structure upon heating.

MATERIALS AND METHODS

Cloning of the psbO Gene. The preparation of cDNA of *T. elongatus* was carried out as described (*40*). For amplification of cDNA encoding recPsbO, two oligonucleotide primers were synthesized, 5′-CATATGGCAAAACAGACTTTAACCTATGACG-3′ and 5′-GGATCCCCTAGGCAGGTTCGATGCTG-3′ (Eurogentec, Cologne, Germany). On the basis of the sense strand of *psbO*, the 5′-coding region for the N-terminal signal sequence was truncated and an *Nde*I restriction site was generated at the start codon (underlined in the sequence). The antisense strand contained a *Bam*HI endonuclease cleavage site two nucleotides downstream from the stop codon (underlined in the sequence). The fragment of the coding region was PCR-amplified and cloned into vector pGEM-T (Promega, Madison, WI). The correctness of the DNA insert was verified by sequencing and after insertion cloned into the expression vector pET11a (Novagen, Madison, WI). The latter was transformed into *E. coli* strain BL21(DE3) (Novagen).

Expression and Purification of recPsbO. The expression and purification of recPsbO was carried out as described (*41*) with some modifications. The culture was induced by adding IPTG to a final concentration of 1 mM. The cells were harvested after 4 h by centrifugation at 6000*g* for 30 min. Cells were opened by osmotic shock; the cell extract was centrifuged at 13000*g* for 30 min and the supernatant filtered through 0.22 μm pore membranes. The protein was loaded onto a DEAE Macroprep column (Biorad, Hercules, CA) equilibrated with buffer A (50 mM MES−NaOH, pH 6.5, 25 mM NaCl). Applying a linear salt gradient (25 mM to 323 mM NaCl), recPsbO eluted at 153 mM NaCl. The fractions containing recPsbO were pooled, dialyzed against buffer A overnight, and loaded onto a Resource Q column (Pharmacia, Uppsala, Sweden) equilibrated with buffer A. A linear gradient was performed as for the DEAE Macroprep column. Fractions containing further purified recPsbO were pooled, concentrated using Amicon Ultra-30 (Millipore, Bedford, MA), and loaded on a Superdex-75 16/60 column (Pharmacia) equilibrated with buffer B (50 mM MES−NaOH, pH 6.5, 100 mM NaCl). Protein purity was tested by SDS−PAGE (*42*) and silver staining (*43*). Protein concentrations were determined spectrophotometrically (λ = 595 nm) using Coomassie G250 (*44*). After electroblotting on polyvinylidene difluoride membranes (Optibran BA S 83, Roth, Karlsruhe, Germany), using a buffer system as described (*45*), immunodetection and visualization of the bands were performed using antibodies raised against polyclonal spinach PsbO. For matrix assisted laser desorption ionization time of flight mass spectrometry (MALDI-TOF MS), samples were diluted with 40% acetonitrile/0.1% trifluoroacetic acid and mixed with sinapinic acid as matrix. Mass standards of cytochrome *c* and myoglobin were used to calibrate the Kompact MALDI II (Shimadzu, Duisburg, Germany) instrument.

PSII Preparation and Reconstitution. T. elongatus was grown at 55 °C, and PSII was isolated and purified as described (*46*). The PSII complexes were used at a Chl*a* concentration of 4 mM as determined spectroscopically (*47*). Wt PsbO was extracted from PSII complexes by incubation on ice for 30 min with buffer in a final concentration of 2.6 M urea, 0.2 M NaCl, and 13 mM MES−NaOH (pH 6.0) (*48*). The detached extrinsic subunits were removed by ultrafiltration with Amicon Ultra-100 (Millipore, Bedford, MA). Supernatant and flow-through were tested by SDS−PAGE and Western blotting for their content of wt PsbO.

For reconstitution, recPsbO was dialyzed against 10 mM NaCl, 10 mM $MgCl_2$, 5 mM $CaCl_2$, and MES−NaOH (pH 6.0) and incubated in molar excess with PsbO-depleted PSII in the dark on ice for 30 min. The light-induced oxygen-evolving activity was measured using a Clark-type electrode (*49*) of native PSII complexes (positive control), of extracted, but not reconstituted PSII complexes (negative control), and of PSII complexes reconstituted with recPsbO in the presence of 2 mM $K_3[FeCN]_6$ and to 0.2 mM phenyl-*p*-benzoquinone as electron acceptors. The buffer contained 20 mM MES−NaOH, pH 6.4, 5 mM $CaCl_2$, and measurements were performed at Chl*a* concentrations of 20−50 μM. Excitation was performed with repetitive 1 Hz flashes from a xenon flash lamp or with saturating continuous white light from a tungsten lamp passing through a heat filter. Maximally we could reconstitute 60−70% of the activity of native PSII core complexes (2200−3700 μmol O_2 (mg Chl*a* h)$^{-1}$; 37−70 Chl*a* (0.25 O_2 flash)$^{-1}$). The presence of recPsbO in all samples was identified by Western blotting (*45*) and immunodecoration using polyclonal anti PsbO. As a loss of Mn ions during the extraction of the extrinsic subunits cannot be excluded, the Mn content of all probes was determined by atom absorption spectroscopy (AAnalyst 800; Perkin-Elmer, BO) (*46*).

UV−CD Spectropolarimetry. For CD spectropolarimetry, recPsbO samples (0.2 mg/mL) were extensively dialyzed against 20 mM KH_2PO_4 (pH 6.5). CD spectra were recorded using a JASCO J600 spectropolarimeter (Gross-Umstadt, Germany) with an RC 6 thermostat (Lauda, Lauda-Königshofen, Germany) that was calibrated with D-camphor-10-sulfonic acid. The samples were allowed to equilibrate at a given temperature for 10 min. The optical path length was 0.1 cm, and data were collected using a scan speed of 50 nm/min. A buffer CD spectrum was recorded and subtracted from all protein spectra that were recorded 5 times and averaged. CD spectra were analyzed using the program K2 (*50*). This program uses a neural network to align the spectrum to given comparative spectra.

FTIR Spectroscopy. The freshly purified recPsbO samples were concentrated to 25.6 mg/mL and dialyzed extensively against D_2O (Sigma-Aldrich, Germany; 99.9% purity) containing 50 mM MES−NaOD (pD 6.0), 6 mM NaCl, and 1 mM ethylene glycol bis(β-aminoethyl ether)-*N*,*N*,*N*′,*N*′-tetraacetic acid (EGTA) or 1 mM $CaCl_2$, respectively, before use. Due to the pH sensitivity of PsbO (*9*, *13*), the pD was adjusted with NaOD to pD 6 (pD = pH + 0.5 pH units). A 10 μL sample was pipetted into an infrared cell with CaF_2 windows and a 23 μm Teflon spacer and placed into a Bruker IFS 66 FTIR spectrometer equipped with a liquid N_2 cooled MCT detector. For each sample 200 interferograms were added and averaged. As reference spectrum the buffer solution was measured under identical conditions and subtracted from the individual protein spectra. The instrument was continuously purged with dry air to prevent spectral contributions due to atmospheric water vapor. A water vapor spectrum was recorded using the same instrumental parameters and interactively subtracted from the buffer-corrected spectrum until a flat baseline resulted between 1715 and 1745 cm^{-1} (see Supporting Information).

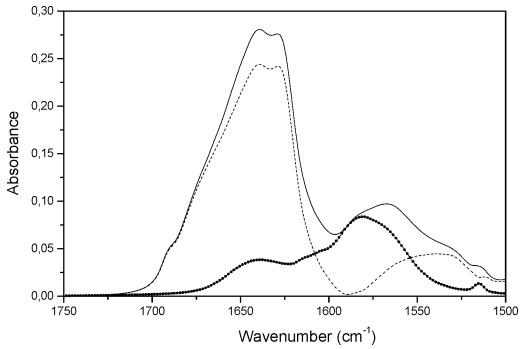

FIGURE 1: FTIR spectra of recPsbO (0.2 mg/mL) in D_2O at pD 6.0 in the presence of 1 mM Ca^{2+}. For experimental conditions, see Materials and Methods. Original spectrum (solid line), spectrum for the side chains (dotted line), and spectrum with side chain correction (dashed line).

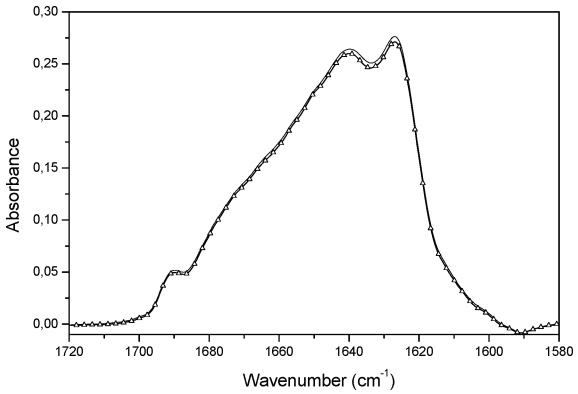

FIGURE 2: Comparison of deconvoluted FTIR spectra in the presence of 1 mM Ca^{2+} at pD 6.0 and line with triangles in the presence of 1 mM EGTA at pD 6.0. For experimental conditions, see Materials and Methods.

RESULTS

recPsbO was expressed and purified as described in Materials and Methods. recPsbO appeared as a single band on silver stained SDS−polyacrylamide gels (not shown). Edman degradation revealed the correct protein sequence of the in frame translated *psbO*. recPsbO eluted as a monomer from the gel filtration column, and by MALDI-TOF MS a molecular mass of 26822 Da was determined, which is in excellent agreement with the calculated mass (26824 Da) (*51*). Spectroscopic experiments in the presence of Ca^{2+} or EGTA were carried out with freshly isolated protein samples of the same preparation.

FTIR Spectra of recPsbO in the Presence and Absence of Ca^{2+} and Secondary Structure Content. The FTIR spectrum of recPsbO in the amide I′ region and the calculated amino acid side chain absorption spectrum between 1500 and 1750 cm^{-1} are presented in Figure 1 and Figure S1 of the Supporting Information. Prior to any further analysis by deconvolution and fitting, the side chain spectrum was subtracted. In the recPsbO FTIR spectrum the amide I′ band is centered at about 1630 cm^{-1}, characteristic for proteins with a high β-sheet secondary structure content (*52*).

Figure 2 and Figure S2 of the Supporting Information show the original and deconvoluted FTIR spectra in the 1580−1720 cm^{-1} region, for recPsbO in D_2O in the presence of Ca^{2+} and EGTA exhibiting two maxima at 1640 and 1625 cm^{-1} for the amide band I′. The deconvoluted spectra showed no significant differences in the spectra of recPsbO in the

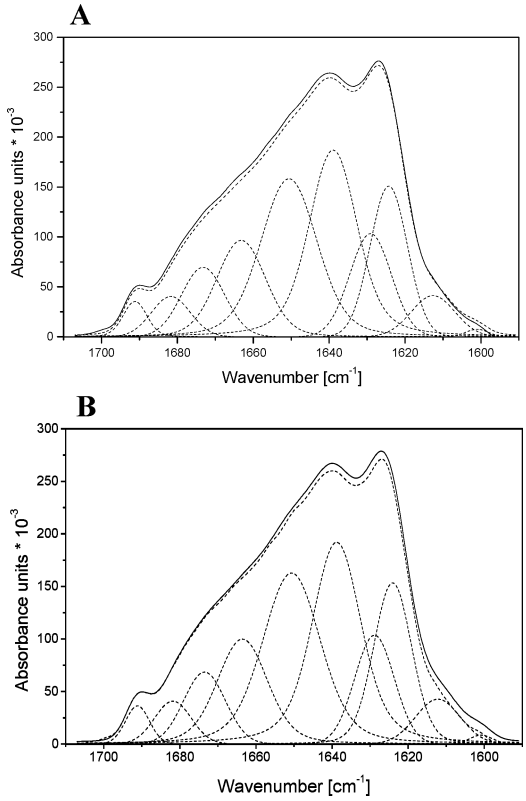

FIGURE 3: Fitted self-deconvoluted amide I′ bands of recPsbO in D_2O pH 7.0. Solid lines represent experimental spectra and dashed lines individual Gaussian components. (A) recPsbO in the presence of 1 mM Ca^{2+}. (B) recPsbO in the presence of 1 mM EGTA.

Table 1: Amide I′ Component Bands, Relative Integrated Intensities (Population), and Secondary Structure Assignments for recPsbO in 50 mM MES−NaOD (pD 6.0), 6 mM NaCl, and 1 mM $CaCl_2$ or 1 mM EGTA, Respectively[a]

+$CaCl_2$		+EGTA		
position (cm^{-1})	population (%)	position (cm^{-1})	population (%)	assignment
1601	0.4	1601	0.4	Arg side chain
1613	4.2	1612	4.2	β-sheet
1624	13.2	1624	13.8	β-sheet
1629	10.1	1629	9.2	β-sheet
1639	24.4	1639	24.7	irregular
1651	23.0	1651	23.6	α-helix
1663	11.8	1664	12.4	turns, loops
1673	7.1	1674	6.4	turns, loops
1682	3.7	1682	3.3	turns, β-sheet
1691	2.1	1691	2.0	β-sheet

[a] For experimental conditions, see Materials and Methods

presence and absence of Ca^{2+} (see Supporting Information). The fitted deconvoluted spectra of recPsbO in the presence of Ca^{2+} and EGTA collected at 27 °C are shown in Figure 3A and Figure 3B, and the position and population of 10 bands are given in Table 1. All band parameters were varied during the fitting, and different start parameters gave the same results. The components of the amide I′ band are designated to a certain secondary structure type according to the assignment from previously published FTIR data of different other proteins (*52*−*56*). Infrared vibration bands in the 1658−1649 cm^{-1} region generally correspond to α-helical structures. Vibrations in the 1637−1620 cm^{-1} region are assigned to β-sheet structures. A second vibrational region at higher wavenumbers, 1690−1675 cm^{-1}, also corresponds to β-sheet structures. Turn structures show signals between 1675 and 1660 cm^{-1} together with stable loops and especially β-turn signals partially overlap with the β-sheet signal around 1979 cm^{-1}. Irregular structures are generally assigned to the region between 1645 and 1640 cm^{-1}.

Table 2: Secondary Structure Prediction for recPsbO as Determined by FTIR Spectroscopy

secondary structure	Ca^{2+} population (%)	EGTA population (%)
β-sheet	33.3	32.5
nonordered	24.8	25.1
α-helix	23.0	23.6
turns, loops	18.9	18.8

In the amide I′ spectrum of recPsbO in D_2O containing buffer in the presence of Ca^{2+} (see Materials and Methods) an α-helical component at 1651 cm^{-1} could be observed. The integrated intensity of this band represents 23.0% of the amide I′ band area. The bands at 1612, 1624, 1629, 1682, and 1691 cm^{-1} are assigned to β-strands, and the sum of the integrated intensities of these five bands suggests a β-sheet content of 33.3% (Table 2) similar to data from Shutova et al. (*9*). If the integrated intensities of the β-turn features at 1664 and 1674 cm^{-1} (18.9%) are added, this results in a total β-structure content of 52.4%. A band at 1601 cm^{-1} having a very small population of 0.4% was not assigned very likely corresponding to arginine side chain absorptions, which are not completely compensated. The remaining component at 1639 cm^{-1} assigned to irregular (non- or disordered) structure contributes to an integrated intensity of 25.1%. However, signals at 1664 and 1674 cm^{-1} can be assigned to β-turn as well as to loop structures, resulting in an irregular protein content of 33.9% and reducing the β-structure content to 32.5% (Table 2). Independent of the assignments of the 1664 and 1674 cm^{-1} bands, the infrared data for recPsbO in the presence of Ca^{2+} indicate a high content of β-sheet structure of about 33%. As a second major component irregular structural elements are identified. As suggested by the similar shape of the recPsbO FTIR amide I′ spectrum in the presence of EGTA, the positions of the bands and the integrated intensities showed no significant changes compared to recPsbO in the presence of Ca^{2+} (Table 1).

CD Spectra of recPsbO, Secondary Structure Determination, and Thermal Denaturation. The secondary structure content of recPsbO was also investigated by CD spectropolarimetry at pH 6.5. Figure 4 shows typical CD spectra of recPsbO between 200 and 260 nm. A buffer spectrum was recorded with the same instrumental parameters and subtracted from each original protein spectrum. The molar ellipticity (Θ) was computed from the original CD reading using the concentration of amino acid residues and the path length. On the basis of the ellipticities between 200 and 240 nm the secondary structure content was predicted yielding a high content of β-sheet structure and a low contribution of α-helices (Table 3) being consistent with previous investigations on cyanobacterial wt PsbO (*10*).

Following the thermal unfolding of recPsbO far-UV CD spectra were recorded in the range of 25−95 °C and corrected for buffer effects (Figure 4A). A temperature-

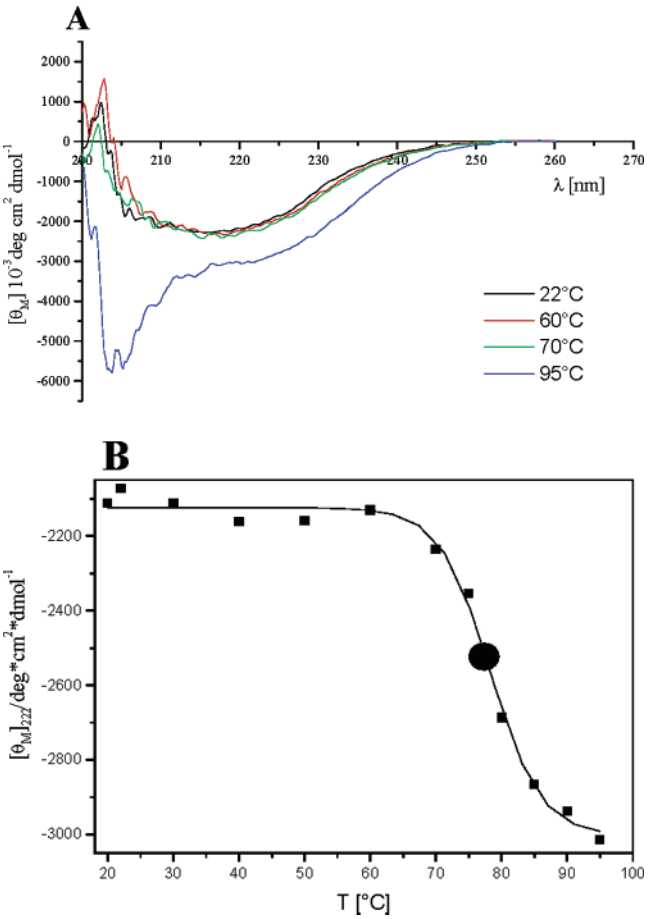

FIGURE 4: (A) CD spectra of recPsbO (0.2 mg/mL) in 20 mM K_2HPO_4 (pH 6.5) recorded at different temperatures (°C), see inset. Each sample was equilibrated for 10 min at the given temperature. (B) Temperature dependence of the negative Θ at 222 nm, taken from spectra as measured in Figure 4A. The inflection point is indicated by a black dot.

Table 3: Predicted Secondary Structure Components of recPsbO Determined by Far UV CD Spectroscopy at Two Different Temperatures and of PsbO Associated with PSII

secondary structure	25 °C population (%)[a]	95 °C population (%)	PSII associated PsbO[b]
β-sheet	43	48	44
irregular	48	48	48
α-helix	8	4	8

[a] 1% of the population at 25 °C could not be assigned to any secondary structure element. [b] According to the PDB entry 1S5L (*16*) and see Supporting Information.

dependent transition of recPsbO above 65 °C indicated by an increase of the negative Θ was observed. This suggests an atypical unfolding without any loss of secondary structure. Analyzing the unfolding of recPsbO upon heating in more detail, the Θ at 222 nm was plotted as a function of temperature (Figure 4B). Independent reproducible measurements showed sigmoidal curves with a transition point at 76 °C. While the Θ at 222 nm suggests an increase in secondary structure, a new negative Cotton effect is observed at 204 nm with an Θ of −5700. Since a minimum in the 200 nm region is usually attributed to random coil, this could be due to a thermally induced aggregation of recPsbO.

The observed thermal denaturation was partially reversible: After heating recPsbO to 95 °C and then cooling to 22 °C its CD spectrum represents 89% complete refolding. Although we obtained sigmoidal structural transition curves for recPsbO, no significant cooperativity in its unfolding pattern could be observed since the range over which the transition occurs is very broad (>30 °C). This is consistent with investigations on the spinach protein (*6*, *9*) suggesting a relatively loose folding of PsbO in solution.

DISCUSSION

Spectroscopic studies have been widely used for gaining information on the structural characteristics of wt PsbO from cyanobacteria and plants. To ensure that the recombinant protein is correctly folded, UV−CD and FTIR spectroscopic studies allow estimation of its secondary structure content (*52*, *54*) and monitoring of overall structural changes upon cofactor binding or chemical and thermal denaturation (*6*, *57*).

For plant PsbO, spectroscopic studies suggest a mainly β-type protein with a high content of nonordered structure (*6*, *9*, *11*, *38*). Some studies indicate possible Ca^{2+} binding (*58*, *59*) and a transition point at 56 °C (*38*).

In the present study the following questions were addressed: (i) does cyanobacterial recPsbO bind Ca^{2+} and, if so, (ii) do we observe cofactor-dependent conformational changes in the protein backbone, and (iii) does recPsbO reveal a thermostability similar to that of the wt protein?

The secondary structure content of recPsbO was determined by CD, and we obtained similar values as was earlier reported for the wt protein from *Synechococcus elongatus* (*10*). Comparable values for irregular structural elements were calculated for both the recPsbO (48%) and wt protein (43%). For wt PsbO Sonoyama et al. (*10*) obtained 23% β-sheets and 17% β-structures, while we calculated a total amount of 43% β-structural elements, since our prediction algorithm (see Supporting Information) does not distinguish between the relative amounts of β-structures and turns. However, the α-helix content differed significantly for recPsbO (8%) and wt PsbO (17%).

When the secondary structure of recPsbO was examined by FTIR, the prediction of the relative content of its secondary structure also partly agrees with data for the wt protein as described by Sonoyama et al. (*10*). While the contents of α-helices (19% wt versus 23% recPsbO) and turn abundancies (17% wt versus 19% recPsbO) are comparable, our study reveals a higher β-structure content (33% recPsbO versus 24% wt) and a smaller contribution of random coils (25% recPsbO versus 40% wt).

Our data clearly show that, depending on the experimental method applied, the secondary structure determination can vary drastically, especially for the relative amounts of α-helices (8% by UV−CD, 23% by FTIR) and irregular structures (48% by UV−CD, 25% by FTIR). A higher α-helix content and a lower relative amount of random coils were also observed for spinach PsbO, when FTIR studies were compared with those using CD (*8*, *9*, *11*). Marked differences in the results of secondary structure analyses performed by CD or FTIR spectroscopy were also reported for other proteins (*60*). These may be explained by the different parameters of secondary structures, which are measured using both techniques. FTIR monitors amide group hydrogen bonding whereas CD reflects torsion angles.

Taken together, our predictions confirm previous reports that PsbO has mainly a β-type structure and a high percentage of random coils (*8*−*10*). This is consistent with crystallographic data on the PSII complex in which PsbO seems to form a β-barrel-like structure (*16*−*18*, *23*). However, the relative amount of irregular structure seems to be much less pronounced in the plant protein when compared with that of thermophilic cyanobacteria. This difference could imply a more flexible structure in cyanobacterial PSII leading to higher thermal stability found for the prokaryotic PsbO by UV−CD spectropolarimetry. As for the wt protein, significant structural changes occurred at temperatures ≥76 °C compared to spinach PsbO, which unfolds at about 50 °C. The transition point for cyanobacterial PsbO at 76 °C is of particular interest, since the PSII holocomplex reveals a similar behavior (J. Frank, A. Zouni, J. Kern, K.-D. Irrgang, unpublished results) supporting previous observations that PsbO is involved in mediating the thermostability of PSII (*6*, *39*, *61*, *62*).

Summarizing our findings, we suggest that PsbO does not have a very rigid structure and its intrinsic flexibility allows it to cope with extreme temperature increases without irreversible structural alterations. These results are consistent with the hypotheses proposed for isolated PsbO attaining either a natively unfolded structure (*6*) or a molten globule (*14*) in solution. It is highly likely that the PsbO structure in solution differs from that within the PSII holocomplex (Table 3) due to interaction of this subunit with membrane intrinsic and extrinsic proteins. This is in line with conclusions from recent structural studies (*15*−*17*).

Several studies showed that Ca^{2+} is an essential cofactor for the oxygen-evolving capability of PSII from both cyanobacteria and higher plants (*59*, *63*−*68*), although there are significant differences in the requirement for this bivalent cation and Cl^- (*68*). The PsbO protein was suggested to directly bind Ca^{2+} in plant PSII (*37*, *65*, *69*); however, the binding constants for Ca^{2+} are 10 times lower when compared to those of other typical Ca^{2+} binding proteins (*57*, *70*). PsbO was proposed to indirectly provide an appropriated ionic environment for the Mn cluster, whereas other investigations rather do not support the view that PsbO interacts with Ca^{2+} (*36*). Recently, Ca^{2+}-dependent conformational changes have been monitored for the plant protein by applying FTIR spectroscopy (*38*). Using a similar experimental setup we could not obtain any evidence for Ca^{2+}-induced structural changes in the cyanobacterial PsbO. These results could be confirmed by UV−CD spectropolarimetry. Therefore the following questions arise: Could the different properties of cyanobacterial versus plant PsbO be attributed to slightly variant primary structures and folding patterns leading in turn to different thermostabilities and to slightly different modes of action? Heredia and de Las Rivas (*38*) suggested that a Ca^{2+}-induced structural modification might facilitate its binding to PSII. However, our data show that no significant conformational change occurs upon Ca^{2+} addition, supporting the view that Ca^{2+} is not bound to the protein before it associates to PSII. Since bivalent metal ions are mainly coordinated by carboxylate groups of Glu or Asp, alterations in the FTIR spectra can be expected even though the overall secondary structure content does not change. For example, the asymmetric stretch mode of COO^- has been shown to act as a marker band for metal binding (*71*). Since no marker band shifts could be observed in our experimental data, cyanobacterial PsbO in solution probably does not specifically bind Ca^{2+} ions. It is important to emphasize that to the best of our knowledge Ca^{2+} binding to PsbO was only identified for the protein from higher plants (*37*, *38*, *58*, *59*, *69*) and not from cyanobacteria. In plant PSII at least two different Ca^{2+} binding sites occur with variant affinities in contrast to that of cyanobacteria (*66*, *67*) (see Supporting Information). The results of our spectroscopic studies are in line with X-ray diffraction data measured beyond the Mn-edge on intact PSII (*16*, *17*), as no anomalous signal was observed at a position equivalent to a heavy atom (Cd^{2+}) binding site in close vicinity to PsbO described in the 3.8 Å structure (*23*). However, since the heteronuclear (Mn_4)Ca cluster (*72*) is probably mainly coordinated by subunit D1 (*16*, *17*), it appears that PsbO serves to exclude water or to contribute only marginally to cation binding. In addition, we cannot exclude that conformational changes most likely occurring upon binding of PsbO to the loop regions of membrane-intrinsic PSII core subunits (but see ref *12*) could create Ca^{2+} binding sites at low−intermediate affinity (mM−μM range) in agreement with Ca^{2+} determinations by atom absorption spectroscopy on the spinach protein (unpublished results).

ACKNOWLEDGMENT

We are grateful to A. Wilde for providing cDNA and help in cloning, to D. DiFiore, C. Lüneberg, Dr. A. Zouni, and Dr. J. Kern for preparation of PSII, to A. Chieduch for technical assistance, to Dr. W. Schröder for N-terminal sequencing, and to Dr. C. Kannicht for recording the MALDI-TOF MS spectra. Thanks are also expressed to Dr. J. Biesiadka for encouragement.

SUPPORTING INFORMATION AVAILABLE

Analysis of CD and FTIR spectra, FTIR spectra of recPsbO (Figures S1 and S2), secondary structure content of associated PsbO, and discussion of Ca^{2+} binding sites within plant PSII. This material is available free of charge via the Internet at http://pubs.acs.org.

REFERENCES

1. Debus, R. J. (1992) The manganese and calcium ions of photosynthetic oxygen evolution, *Biochim. Biophys. Acta 1102*, 269−352.
2. de Las Rivas, J., Balsera, M., and Barber, J. (2004) Evolution of oxygenic photosynthesis: genome-wide analysis of the OEC extrinsic proteins, *Trends Plant Sci. 9*, 18−25.
3. Seidler, A. (1996) The extrinsic polypeptides of Photosystem II, *Biochim. Biophys. Acta 1277*, 35−60.
4. Bricker, T. M., and Frankel, L. K. (1998) The structure and function of the 33 kDa extrinsic protein of photosystem II: a critical assessment, *Photosynth. Res. 56*, 157−173.
5. Tohri, A., Suzuki, T., Okuyama, S., Kamino, K., Motoki, A., Hirano, M., Ohta, H., Shen, J. R., Yamamoto, Y., and Enami, I. (2002) Comparison of the structure of the extrinsic 33 kDa protein from different organisms, *Plant Cell Physiol. 43*, 429−439.
6. Lydakis-Simantiris, N., Hutchison, R. S., Betts, S. D., Barry, B. A., and Yocum, C. F. (1999) Manganese stabilizing protein of photosystem II is a thermostable, natively unfolded polypeptide, *Biochemistry 38*, 404−414.
7. Motoki, A., Usui, M., Shimazu, T., Hirano, M., and Katoh, S. (2002) A domain of the Mn-stabilizing protein from *Synechococcus elongatus* involved in functional binding to photosystem II, *J. Biol. Chem. 23*, 23.

8. Xu, Q., Nelson, J., and Bricker, T. M. (1994) Secondary structure of the 33 kDa, extrinsic protein of Photosystem II: a far-UV circular dichroism study, *Biochim. Biophys. Acta 1188*, 427−431.
9. Shutova, T., Irrgang, K.-D., Shubin, V., Klimov, V. V., and Renger, G. (1997) Analysis of pH-induced structural changes of the isolated extrinsic 33 kilodalton protein of photosystem II, *Biochemistry 36*, 6350−6358.
10. Sonoyama, M., Motoki, A., Okamoto, G., Hirano, M., Ishida, H., and Katoh, S. (1996) Secondary structure and thermostability of the photosystem II manganese-stabilizing protein of the thermophilic cyanobacterium *Synechococcus elongatus*, *Biochim. Biophys. Acta 1297*, 167−170.
11. Ahmed, A., Tajmir-Riahi, H. A., and Carpentier, R. (1995) A quantitative secondary structure analysis of the 33 kDa extrinsic polypeptide of photosystem II by FTIR spectroscopy, *FEBS Lett. 363*, 65−68.
12. Svensson, B., Tiede, D. M., Nelson, D. R., and Barry, B. A. (2004) Structural studies of the manganese stabilizing subunit in photosystem II, *Biophys. J. 86*, 1807−1812.
13. Weng, J., Tan, C., Shen, J. R., Yu, Y., Zeng, X., Xu, C., and Ruan, K. (2004) pH-induced conformational changes in the soluble manganese-stabilizing protein of photosystem II, *Biochemistry 43*, 4855−4861.
14. Shutova, T., Irrgang, K.-T., Klimov, V. V., and Renger, G. (2000) Is the manganese stabilizing 33 kDa protein of photosystem II attaining a "natively unfolded" or "molten globule" structure in solution? *FEBS Lett. 467*, 137−140.
15. Nowaczyk, M., Berghaus, C., Stoll, R., and Rögner, M. (2004) Preliminary structural characterisation of the 33 kDa protein (PsbO) in solution studied by site-directed mutagenesis and NMR spectroscopy, *Phys. Chem. Chem. Phys. 6*, 4878−4881.
16. Ferreira, K. N., Iverson, T. M., Maghlaoui, K., Barber, J., and Iwata, S. (2004) Architecture of the photosynthetic oxygen-evolving center, *Science 303*, 1831−1838.
17. Biesiadka, J., Loll, B., Kern, J., Irrgang, K.-D., and Zouni, A. (2004) Crystal structure of cyanobacterial photosystem II at 3.2 Å resolution: a closer look at the Mn-cluster, *Phys. Chem. Chem. Phys. 6*, 4733−4736.
18. Kamiya, N., and Shen, J. R. (2003) Crystal structure of oxygen-evolving photosystem II from *Thermosynechococcus vulcanus* at 3.7 Å resolution, *Proc. Natl. Acad. Sci. U.S.A. 100*, 98−103.
19. Odom, W. R., and Bricker, T. M. (1992) Interaction of CPa-1 with the manganese-stabilizing protein of photosystem II: identification of domains cross-linked by 1-ethyl-3-[3-(dimethylamino)propyl]carbodiimide, *Biochemistry 31*, 5616−5620.
20. Enami, I., Kaneko, M., Kitamura, N., Koike, H., Sonoike, K., Inoue, Y., and Katoh, S. (1991) Total immobilisation of the extrinsic 33-kDa protein in spinach photosystem II membrane preparations. Protein stoichiometry and stabilisation of oxygen evolution, *Biochim. Biophys. Acta 1060*, 224−232.
21. Hillier, W., and Wydrzynski, T. (1993) Increase in peroxide formation by the Photosystem II oxygen evolving reactions upon removal of the extrinsic 16, 22 and 33 kDa proteins are reversed by $CaCl_2$ addition, *Photosynth. Res. 38*, 417−423.
22. Cole, J. L., Yachandra, V. K., McDermott, A. E., Guiles, R. D., Britt, R. D., Dexheimer, S. L., Sauer, K., and Klein, M. P. (1987) Structure of the manganese complex of photosystem II upon removal of the 33-kilodalton extrinsic protein: an X-ray absorption spectroscopy study, *Biochemistry 26*, 5967−5973.
23. Zouni, A., Witt, H. T., Kern, J., Fromme, P., Krauss, N., Saenger, W., and Orth, P. (2001) Crystal structure of photosystem II from *Synechococcus elongatus* at 3.8 Å resolution, *Nature 409*, 739−743.
24. Krieger, A. (1995) Effect of the Ca^{2+} channel activator CGP 28392 on reactivation of oxygen evolution of Ca^{2+}-depleted photosystem II, *FEBS Lett. 367*, 173−176.
25. Anderson, J. M. (2001) Does functional photosystem II complex have an oxygen channel? *FEBS Lett. 488*, 1−4.
26. Ono, T. A., and Inoue, Y. (1983) Mn-preserving extraction of 33-, 24- and 16-kDa proteins from O_2-evolving PSII particles by divalent salt-washing, *FEBS Lett. 164*, 255−260.
27. Miyao, M., and Murata, N. (1984) Role of the 33 kDa polypeptide in preserving Mn in the photosynthetic oxygen-evolution, *FEBS Lett. 170*, 350−354.
28. Miyao, M., Murata, N., Lavorel, J., Maison-Peteri, B., Boussac, A., and Etienne, A. L. (1987) Effect of the 33 kDa protein on the S-state transitions in photosynthetic oxygen evolution, *Biochim. Biophys. Acta 890*, 151−159.
29. Razeghifard, M. R., Wydrzynski, T., Pace, R. J., and Burnap, R. L. (1997) $Y_z^{\bullet}$ reduction kinetics in the absence of the manganese-stabilizing protein of photosystem II, *Biochemistry 36*, 14474−14478.
30. Burnap, R. L., Qian, M., and Pierce, C. (1996) The manganese stabilizing protein of photosystem II modifies the *in vivo* deactivation and photoactivation kinetics of the H_2O oxidation complex in *Synechocystis sp.* PCC 6803, *Biochemistry 35*, 874−882.
31. Philbrick, J. B., Diner, B. A., and Zilinskas, B. A. (1991) Construction and characterization of cyanobacterial mutants lacking the manganese-stabilizing polypeptide of photosystem II, *J. Biol. Chem. 266*, 13370−13376.
32. Mayes, S. R., Cook, K. M., Self, S. J., Zhang, Z., and Barber, J. (1991) Deletion of the gene encoding the PSII 33kDa protein from *Synechocystis* PCC 6803 does not inactivate water splitting but increases vulnerability to photoinhibition, *Biochim. Biophys. Acta 1060*, 1−12.
33. Burnap, R. L., and Sherman, L. A. (1991) Deletion mutagenesis in *Synechocystis* sp. PCC 6803 indicates that the Mn-stabilizing protein of photosystem II is not essential for O_2 evolution, *Biochemistry 30*, 440−446.
34. Miyao, M., and Murata, N. (1983) Partial reconstitution of photosynthetic oxygen evolution system by rebinding of the 33 kDa polypeptide, *FEBS Lett. 164*, 375−378.
35. Bricker, T. M. (1992) Oxygen evolution in the absence of the 33-kilodalton manganese-stabilizing protein, *Biochemistry 31*, 4623−4628.
36. Seidler, A., and Rutherford, A. W. (1996) The role of the extrinsic 33 kDa protein in Ca^{2+} binding in photosystem II, *Biochemistry 35*, 12104−12110.
37. Wales, R., Newman, B. J., Pappin, D., and Gray, J. C. (1989) The extrinsic 33 kDa polypeptide of the oxygen-evolving complex of photosystem II is a putative calcium-binding protein and is encoded by a multi-gene family in pea, *Plant Mol. Biol. 12*, 439−451.
38. Heredia, P., and de Las Rivas, J. (2003) Calcium-dependent conformational change and thermal stability of the isolated PsbO protein detected by FTIR spectroscopy, *Biochemistry 42*, 11831−11838.
39. Pueyo, J. J., Alfonso, M., Andres, C., and Picorel, R. (2002) Increased tolerance to thermal inactivation of oxygen evolution in spinach Photosystem II membranes by substitution of the extrinsic 33-kDa protein by its homologue from a thermophilic cyanobacterium, *Biochim. Biophys. Acta 1554*, 29−35.
40. Chiaramonte, S., Giacometti, G. M., and Bergantino, E. (1999) Construction and characterization of a functional mutant of *Synechocystis* 6803 harbouring a eukaryotic PSII−H subunit, *Eur. J. Biochem. 260*, 833−843.
41. Seidler, A., and Michel, H. (1990) Expression in *Escherichia coli* of the *psbO* gene encoding the 33 kd protein of the oxygen-evolving complex from spinach, *EMBO J. 9*, 1743−1748.
42. Laemmli, U. K. (1970) Cleavage of structural proteins during the assembly of the head of bacteriophage T4, *Nature 227*, 680−685.
43. Heukeshoven, J., and Dernick, R. (1985) Simplified method for silver staining of proteins in polyacrylamide gels and the mechanism of silver staining, *Electrophoresis 6*, 1103−1121.
44. Bradford, M. M. (1976) A rapid and sensitive method for the quantitation of microgram quantities of protein utilizing the principle of protein-dye binding, *Anal. Biochem. 72*, 248−254.
45. Towbin, H., Staehelin, T., and Gordon, J. (1979) Electrophoretic transfer of proteins from polyacrylamide gels to nitrocellulose sheets: procedure and some applications, *Proc. Natl. Acad. Sci. U.S.A. 76*, 4350−4354.
46. Kern, J., Loll, B., Lüneberg, C., DiFiore, D., Biesiadka, J., Irrgang, K.-D., and Zouni, A. (2005) Purification, characterisation and crystallisation of photosystem II from *Thermosynechococcus elongatus* cultivated in a new type of photobioreactor, *Biochim. Biophys. Acta 1706*, 147−157.
47. Porra, R. J., Thompson, M. P., and Kriedemann, P. A. (1989) Determination of accurate extinction coefficients and simultaneous equations for assaying chlorophylls *a* and *b* extracted with four different solvents: verification of the concentration of chlorophyll standards by atom absorption spectroscopy, *Biochim. Biophys. Acta 74*, 384−394.
48. Miyao, M., and Murata, N. (1984) Role of the 33 kDa polypeptide in preserving Mn in the photosynthetic oxygen-evolution, *FEBS Lett. 170*, 350−354.

49. Renger, G. (1972) The action of 2-anilinothiophenes as accelerators of the deactivation reactions in the water splitting enzyme system of photosynthesis, *Biochim. Biophys. Acta 256*, 428−439.
50. Andrade, M. A., Chacon, P., Merelo, J. J., and Moran, F. (1993) Evaluation of secondary structure of proteins from UV circular dichroism spectra using an unsupervised learning neural network, *Protein Eng. 6*, 383−390.
51. Miura, K., Shimazu, T., Motoki, A., Kanai, S., Hirano, M., and Katoh, S. (1993) Nucleotide sequence of the Mn-stabilizing protein gene of the thermophilic cyanobacterium *Synechococcus elongatus*, *Biochim. Biophys. Acta 1172*, 357−360.
52. Byler, D. M., and Susi, H. (1986) Examination of the secondary structure of proteins by deconvolved FTIR spectra, *Biopolymers 25*, 469−487.
53. Krimm, S., and Bandekar, J. (1986) Vibrational spectroscopy and conformation of peptides, polypeptides, and proteins, *Adv. Protein Chem. 38*, 181−364.
54. Surewicz, W. K., and Mantsch, H. H. (1988) New insight into protein secondary structure from resolution-enhanced infrared spectra, *Biochim. Biophys. Acta 952*, 115−130.
55. Arrondo, J. L., Young, N. M., and Mantsch, H. H. (1988) The solution structure of concanavalin A probed by FT-IR spectroscopy, *Biochim. Biophys. Acta 952*, 261−268.
56. Prestrelski, S. J., Byler, D. M., and Thompson, M. P. (1991) Infrared spectroscopic discrimination between α- and 3_{10}-helices in globular proteins. Reexamination of Amide I infrared bands of α-lactalbumin and their assignment to secondary structures, *Int. J. Pept. Protein Res. 37*, 508−512.
57. Casal, H. L., Kohler, U., and Mantsch, H. H. (1988) Structural and conformational changes of β-lactoglobulin B: an infrared spectroscopic study of the effect of pH and temperature, *Biochim. Biophys. Acta 957*, 11−20.
58. Kruk, J., Burda, K., Jemiola-Rzeminska, M., and Strzalka, K. (2003) The 33 kDa protein of photosystem II is a low-affinity calcium- and lanthanide-binding protein, *Biochemistry 42*, 14862−14867.
59. Zhang, L. X., Liang, H. G., Wang, J., Li, W. R., and Yu, T. Z. (1996) Fluorescence and Fourier-transform infrared spectroscopic studies on the role of disulfide bond in calcium binding in the 33 kDa protein of Photosystem II, *Photosynth. Res. 48*, 379−384.
60. Hadden, J. M., Bloemendal, M., Haris, P. I., Srai, S. K., and Chapman, D. (1994) Fourier transform infrared spectroscopy and differential scanning calorimetry of transferrins: human serum transferrin, rabbit serum transferrin and human lactoferrin, *Biochim. Biophys. Acta 1205*, 59−67.
61. Nishiyama, Y., Hayashi, H., Watanabe, T., and Murata, N. (1994) Photosynthetic Oxygen evolution is stabilized by cytochrome *c*550 against heat inactivation in *Synechococcus* sp. PCC 7002, *Plant Physiol. 105*, 1313−1319.
62. Kimura, A., Eaton-Rye, J. J., Morita, E. H., Nishiyama, Y., and Hayashi, H. (2002) Protection of the oxygen-evolving machinery by the extrinsic proteins of photosystem II is essential for development of cellular thermotolerance in Synechocystis sp. PCC 6803, *Plant Cell Physiol. 43*, 932−938.
63. Ghanotakis, D. F., Topper, J. N., Babcock, G. T., and Yocum, C. F. (1984) Water-soluble 17 and 23 kDa polypeptides restore oxygen evolution activity by creating a high-affinity binding site for Ca^{2+} on the oxidising site of photosystem II, *FEBS Lett. 170*, 169−173.
64. Nakatani, H. Y. (1984) Inhibition of photosynthetic oxygen evolution by calmodulin-type inhibitors and other calcium-antagonists, *Biochem. Biophys. Res. Commun 121*, 626−633.
65. Grove, G. N., and Brudvig, G. W. (1998) Calcium binding studies of photosystem II using a calcium-selective electrode, *Biochemistry 37*, 1532−1539.
66. Ädelroth, P., Lindberg, K., and Andreasson, L. E. (1995) Studies of Ca^{2+} binding in spinach photosystem II using $^{45}Ca^{2+}$, *Biochemistry 34*, 9021−9027.
67. Kashino, Y., Satoh, K., and Katoh, S. (1986) A simple procedure to determine Ca^{2+} in oxygen-evolving preparations from *Synechococcus* sp., *FEBS Lett. 205*, 150−153.
68. Pauly, S., Schlodder, E., and Witt, H. T. (1992) The influence of salts on charge separation ($P680^+Q_A^-$) and water oxidation of Photosystem II complexes from thermophilic cyanobacteria. Active and inactive conformational states of Photosystem II, *Biochim. Biophys. Acta 1099*, 203-210.
69. Webber, A. N., and Gray, J. C. (1989) Detection of calcium binding by Photosystem II polypeptides immobilized onto nitrocellulose membrane, *FEBS Lett. 249*, 79−81.
70. Strynadka, N. C., and James, M. N. (1989) Crystal structures of the helix-loop-helix calcium-binding proteins, *Annu. Rev. Biochem. 58*, 951−998.
71. Nara, M., Tasumi, M., Tanokura, M., Hiraoki, T., Yazawa, M., and Tsutsumi, A. (1994) Infrared studies of interaction between metal ions and Ca(2+)-binding proteins. Marker bands for identifying the types of coordination of the side-chain COO− groups to metal ions in pike parvalbumin (pI = 4.10), *FEBS Lett. 349*, 84−88.
72. Cinco, R. M., Robblee, J. H., Messinger, J., Fernandez, C., McFarlane Holman, K. L., Sauer, K., and Yachandra, V. K. (2004) Orientation of calcium in the Mn_4Ca cluster of the oxygen-evolving complex determined using polarized strontium EXAFS of photosystem II membranes, *Biochemistry 43*, 13271−13282.

BI047614R